Excited State Dynamics of *meso*-Tetra(sulphonatophenyl) Metalloporphyrins

P. J. Gonçalves,*,† L. De Boni,† I. E. Borissevitch,‡ and S. C. Zílio†

Instituto de Física de São Carlos, Universidade de São Paulo, Caixa Postal 369, 13560-970, São Carlos, SP, Brazil, and Departamento de Física e Matemática, FFLCRP, Universidade de São Paulo, Avenida Bandeirantes 3900, 14040-901, Ribeirão Preto, SP, Brazil

Received: January 21, 2008; Revised Manuscript Received: April 10, 2008

The excited state dynamics of Zn^{2+}, Fe^{3+}, and Mn^{3+} *meso*-tetra(sulfonatophenyl) porphyrin complexes were investigated with a Z-scan technique at 532 nm using 70 ps and 120 fs single pulses and 200 ns pulse trains of a Q-switched and mode locked laser. We determined the characteristic interconversion and intersystem crossing times, quantum yields of the excited S_1 state, and $S_1 \rightarrow S_n$ and $T_1 \rightarrow T_n$ transition cross-sections. The ground state cross-sections were obtained using UV−vis absorption spectroscopy, and a five-energy-level diagram was used to yield the photophysical parameters mentioned previously.

Introduction

Porphyrins and their derivatives are characterized by intense optical absorption, high photostability, photodynamic activity, and a high affinity to biological structures, in particular, to malignant tissues. Owing to these characteristics, they are successfully applied in photodynamic therapy (PDT) for cancer treatment.[1,2] When paramagnetic metals (Fe^{3+}, Mn^{3+}, etc.) are incorporated into their structures, they can be used as contrast agents in nuclear magnetic resonance (NMR) tomography for cancer diagnostics.[3,4] The high nonlinear optical susceptibilities and fast response times of metalloporphyrin complexes, arising from two-dimensional conjugated π-electron systems, makes them promising candidates for applications of photonic devices, such as optical limiters and switches.[5–11] However, for the successful development of such devices, it is important to characterize the photophysical parameters of the excited states, which include cross-sections, lifetimes, and quantum yields. The study of ultrafast molecular deactivation is also important to elucidate mechanisms involved in electronic and vibronic excitations, as well as in electron and energy transfers that take part in various processes such as photosynthesis, PDT, and optical limiting.[7–12]

This work reports the photophysical parameters of Zn^{2+}, Fe^{3+}, and Mn^{3+} *meso*-tetra(sulphonatophenyl) ($TPPS_4$) porphyrins obtained through the analysis of optical nonlinearity dynamics. The nonradiative deactivation of Fe^{3+} and Mn^{3+} porphyrin complexes is very fast, and for this reason, we employed a Z-scan technique with 120 fs pulses to achieve the sought parameters. The data obtained were complemented with UV−vis absorption spectroscopy as a way to characterize the ground state cross-sections. We determined the singlet and triplet excited state cross-sections (σ^{S}_{exc} and σ^{T}_{exc}); fluorescence (φ_{fl}), intersystem crossing (φ_{isc}), and internal conversion (φ_{ic}) quantum yields; and characteristic times.

Materials and Methods

Zn^{2+}, Fe^{3+}, and Mn^{3+} $TPPS_4$ porphyrin complexes were purchased from Porphyrin Products Inc. and dissolved in Milli-Q quality water. Experiments with Zn^{2+} and Mn^{3+} complexes were performed at pH 6.8, but since Fe^{3+} $TPPS_4$ is found as a solution of H_2O-Fe^{3+} $TPPS_4$-OH_2 monomers when the pH is less than 7.8 and as H_2O-Fe^{3+} $TPPS_4$-O-Fe^{3+} $TPPS_4$-OH_2 μ-oxo dimers for pH higher than 7.8,[13] the measurements with this complex were carried out at pH 4.0 and 9.0. The concentrations were monitored spectrophotometrically, and the pH values used were achieved by the addition of appropriate amounts of HCl or NaOH stock solutions. The UV−vis spectra were measured with a Beckman DU 640 spectrophotometer. All experiments were performed at room temperature with the samples placed in a 2 mm thick quartz cuvette.

While the ground state absorption and fluorescence lifetime can be obtained by conventional spectroscopic techniques, the determination of the excited state photophysical parameters requires much higher intensities and can be investigated with nonlinear techniques, such as the open aperture Z-scan technique.[14] This basically consists of monitoring the sample transmittance as it translates through the focal plane of a tightly focused laser beam. The open aperture configuration collects all energy transmitted and is sensitive only to nonlinear absorption, not to other nonlinear effects, such as thermal lensing, self-focusing, or stimulated Raman scattering. The usefulness of this technique to study excited state parameters already was demonstrated.[15–19]

In our Z-scan experiments, two pump sources were used. The first was a frequency doubled, Q-switched, and mode-locked Nd:YAG laser, producing pulse trains containing ca. twenty 70 ps pulses at 532 nm, separated by 13 ns intervals and spanning a range of ~200 ns. This light source was applied in two regimes: by exciting the sample with a single pulse extracted from the pulse train under the Q-switch envelope and with the complete pulse train (PTZ-scan technique).[20] In this way, it is possible to study nonlinearities in picosecond and nanosecond timescales, respectively.

The PTZ-scan experimental setup is same as the traditional one, but as the sample is moved along the focal plane, a complete pulse train is acquired, and the amplitudes of each individual pulse in the train are normalized to those obtained when the sample is far from the focus. This procedure gives a set of Z-scan signatures, one for each pulse. For the single pulse Z-scan, a Pockels cell was used to extract a single pulse from

* Corresponding author. Fax: +55-16-3373-8085, ext. 212; e-mail: pablo@ifsc.usp.br.
† Instituto de Física de São Carlos.
‡ Departamento de Física e Matemática.

10.1021/jp800589j CCC: $40.75
Published on Web 06/28/2008

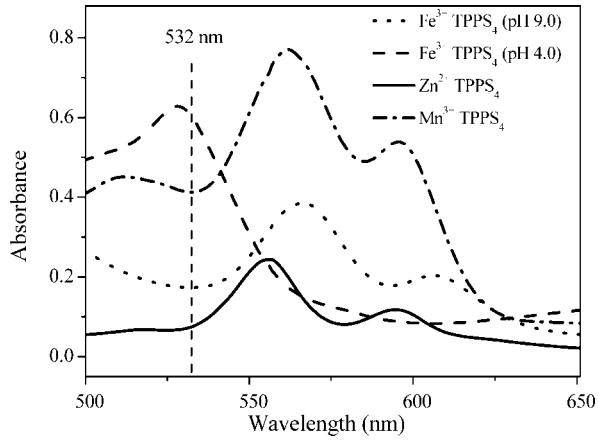

Figure 1. Absorbance spectra of $TPPS_4$ metalloporphyrins.

TABLE 1: Cross-Sections of $S_0 \rightarrow S_1$ (σ_g), $S_1 \rightarrow S_n$ (σ^S_{exc}), and $T_1 \rightarrow T_n$ (σ^T_{exc}) Transitions and Ratios between Them for Studied Compounds[a]

$TPPS_4$	pH	σ_g	σ^S_{exc}	σ^T_{exc}	σ^S_{exc}/σ_g	σ^T_{exc}/σ_g
free base[15]	4.0	0.8 (±0.1)	7.4 (±0.2)	7.6 (±0.2)	9.3 (±0.8)	9.5 (±0.8)
free base[15]	7.0	2.1 (±0.1)	4.7 (±0.2)	3.3 (±0.2)	2.2 (±0.3)	1.6 (±0.2)
Fe^{3+}	4.0	3.7 (±0.1)	3.9 (±0.2)	3.4 (±0.2)	1.1 (±0.1)	0.9 (±0.1)
Fe^{3+}	9.0	0.4 (±0.1)	5.7 (±0.2)	0.9 (±0.1)	14 (±5)	2.3 (±0.9)
Mn^{3+}	6.8	2.3 (±0.1)	4.6 (±0.2)	4.2 (±0.2)	2.0 (±0.2)	1.8 (±0.2)
Zn^{2+}	6.8	1.7 (±0.1)	4.3 (±0.2)	7.2 (±0.2)	2.5 (±0.3)	4.2 (±0.4)

[a] Cross-sections are in units of 10^{-17} cm^2.

the train. For both regimes, the beam was focused onto the quartz cuvette with a $f = 12$ cm lens, resulting in a waist $w_0 = 25$ μm at the focal plane. We used a 10 Hz repetition rate to avoid accumulative thermal nonlinearities.

The second source was an optical parametric amplifier (OPA) operating at 532 nm, pumped by 150 fs pulses at 775 nm from a 1 kHz Ti:sapphire chirped pulse amplified system. This source produced 120 fs pulses, which are quite suitable to study fast nonlinearities associated with excited states as those found in metalloporphyrins. In this case, only one excited state is populated during the pulse, and the populations of other excited states can be neglected.

Results and Discussion

The absorbance spectra of the porphyrin complexes used in this work show Q-bands that can be excited by 532 nm, as depicted in Figure 1. The ground state absorption cross-sections (σ_g) at 532 nm were found through the relation $\sigma_g = 2.3A/NL$, where A is the sample absorbance ($A = -\log_{10}(I/I_0)$), N is the sample concentration (in molecules/vol), and L is the quartz cuvette thickness. The values obtained are shown in Table 1.

Figure 2 shows the Zn^{2+} $TPPS_4$ normalized transmittance as a function of the pulse fluence obtained in the Z-scan experiment with 70 ps single pulses. In general, the population dynamics and photophysics parameters of porphyrins can be determined by means of the five-energy-level diagram shown in the inset of Figure 2. This diagram includes the molecular ground state singlet level (S_0), two excited singlet levels (S_1 and S_n), and two triplet levels (T_1 and T_n). The incidence of an intense resonant light pulse redistributes the population of molecules among the ground and excited states, causing a transient modification of the optical properties of the material. However, since the intersystem crossing time (τ_{isc}) in Zn^{2+} $TPPS_4$ is in the nanosecond range,[21] the triplet state population created

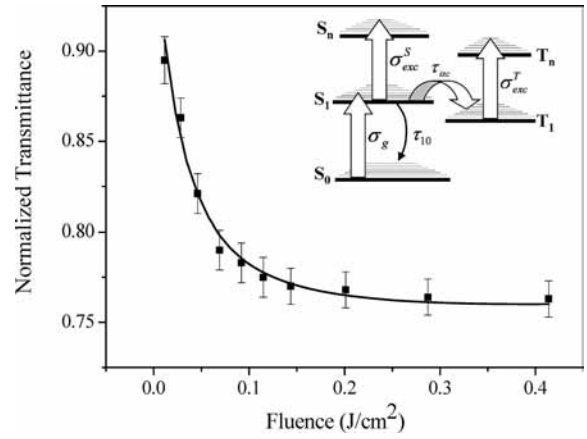

Figure 2. Normalized Zn^{2+} $TPPS_4$ transmittance as function of the single 70 ps pulse fluence. The inset shows the five-energy-level diagram used to determine the excited state dynamics.

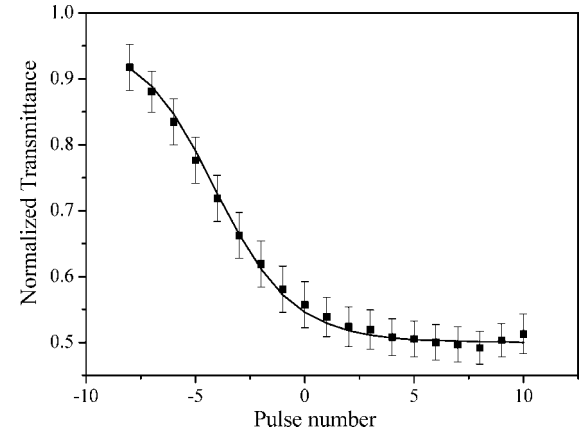

Figure 3. Normalized Zn^{2+} $TPPS_4$ transmittance as a function of pulse number. The solid line results from the fitting procedure described in the text.

during the single pulse can be neglected. This permits the use of a simplified model that includes only three levels of the singlet manifold. As discussed next, the singlet excited state cross-section can be determined by observing the saturation behavior of the normalized transmittance as a function of pulse fluence.

Beer's law equation governing the variation of irradiance along the penetration depth, z, was presented previously as[15]

$$\frac{dI}{dz'} = -\alpha(t)I(t) = -\alpha_0\left\{1 + \left(\frac{\sigma^S_{exc}}{\sigma_g} - 1\right) \times \left(1 - \exp\left\{-\frac{\sigma_g F(t)}{h\nu}\right\}\right)\right\} I(t) \quad (1)$$

where I is the laser irradiance and $F(t) = \int_{-\infty}^{t} I(t)dt$ is its fluence. Since the detector response (~1 ns) in our Z-scan setup is much longer than the pulse duration, we numerically integrated eq 1 over t from $-\infty$ to $+\infty$, over sample thickness L and the transverse profile of the laser beam. The result was normalized to the linearly transmitted energy, $\epsilon = \epsilon_0 \exp\{-\alpha_0 L\}$ and provided the value of σ^S_{exc}.

Figure 3 depicts the accumulative nonlinearity for Zn^{2+} $TPPS_4$ obtained with the PTZ-scan technique, where the strongest pulse in the train was arbitrarily labeled 0. The behavior observed is associated to the progressive long-lived triplet population. In these experiments, the time interval between consecutive pulses in the pulse train (13 ns) is ~8 times longer than τ_{10} (1.7 ns),[21]

meaning that there is enough time between consecutive pulses to partially populate the T_1 state. On the other hand, the Q-switch envelope duration is ~200 ns, which is 10 times shorter than the T_1 state lifetime (≈2 μs in the presence of O_2). Therefore, the T_1 state population increases progressively during the pulse train action, and its depopulation can be ignored.

In this case, it is necessary to use the complete five-energy-level diagram. The rate equations describing the population fractions are

$$\frac{dn_{S_0}}{dt} = -W_{0_1} n_{S_0} + \left(\frac{1}{\tau_{S_1}} - \frac{1}{\tau_{isc}}\right) n_{S_1} \quad (2a)$$

$$\frac{dn_{S_1}}{dt} = W_{0_1} n_{S_0} - \frac{n_{S_1}}{\tau_{S_1}} \quad (2b)$$

$$\frac{dn_{T_1}}{dt} = \frac{n_{S_1}}{\tau_{isc}} \quad (2c)$$

where $W_{0_1} = \sigma_g I/h\nu$ is the one-photon absorption rate and the normalization condition $n_{S_0} + n_{S_1} + n_{T_1} = 1$ applies. The S_1 state lifetime was written as $\tau_{S_1}^{-1} = \tau_{10}^{-1} + \tau_{isc}^{-1}$, where τ_{isc} is the intersystem crossing time and τ_{10}^{-1} contains the contribution of internal conversion (τ_{ic}) and radiative lifetime (τ_r) of the $S_1 \rightarrow S_0$ transition ($\tau_{10}^{-1} = \tau_r^{-1} + \tau_{ic}^{-1}$).

This set of equations was numerically solved by using the temporal intensity pattern of the Q-switched/mode-locked pulse train employed in our Z-scan experiments, with initial conditions $n_{S_0}(-\infty) = 1$ and $n_{S_1}(-\infty) = n_{T_1}(-\infty) = 0$, producing new values for populations at each pulse. This procedure yields the population dynamics necessary to determine the excited state parameters. The time evolution of the absorption can be calculated according to

$$\alpha(t) = -N\left[n_{S_0}\sigma_g + n_{S_1}\sigma^S{}_{exc} + n_{T_1}\sigma^T{}_{exc}\right] \quad (3)$$

Eqs 2a−c and 3were numerically solved using σ_g and $\sigma^S{}_{exc}$ obtained from previous measurements and the value of τ_{S_1} found in the literature.[21] Normalizing the result to the linearly transmitted energy, the values of the intersystem crossing time and triplet excited state absorption cross-section were obtained from the best fitting of the PT Z-scan data, as depicted by the solid line in Figure 3.

Mn^{3+} and Fe^{3+} $TPPS_4$ do not show any accumulative behavior when subjected to the complete pulse train. The nonlinear absorption was observed just when 70 ps and 120 fs single pulses were employed, meaning that their excited singlet state lifetimes are ultrashort. In general, porphyrin complexes with paramagnetic metals have very fast nonradiative relaxation rates,[21,22] and if the pulse duration is longer than the excited state lifetime, there is enough time to populate other excited levels during the pulse action. Therefore, to avoid the triplet state contribution, 120 fs pulses were employed to study the excited singlet cross-section in these complexes because such duration is expected to be shorter than S_1 state lifetimes for Mn^{3+} and Fe^{3+} $TPPS_4$. Since in this case the triplet population can be neglected, the nonlinear absorption signal is attributed only to $S_0 \rightarrow S_1$ and $S_1 \rightarrow S_n$ transitions, and $\sigma^S{}_{exc}$ can be determined with the simplified three-energy-level model giving rise to eq 1. Figure 4 illustrates the normalized transmittance curve obtained by the Z-scan technique with 120 fs pulses in Mn^{3+} $TPPS_4$. The Fe^{3+} $TPPS_4$ sample gives a similar result.

The normalized transmittance observed in Z-scan measurements with single 70 ps pulses depends on the pulse fluence as shown in Figure 5. This result can be explained by considering

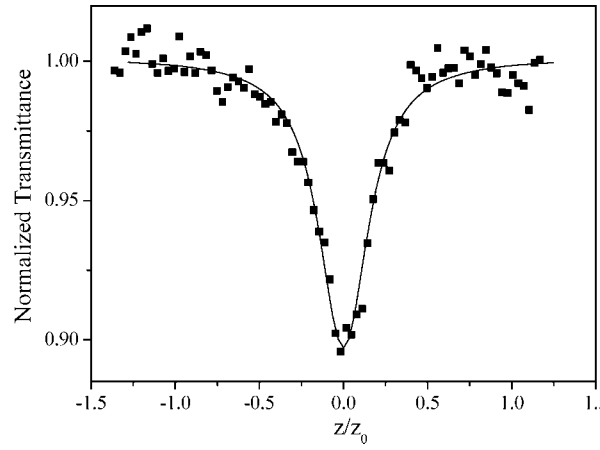

Figure 4. Mn^{3+} $TPPS_4$ normalized transmittance curve obtained with the Z-scan technique with 120 fs pulses. The fitting was used to obtain $\sigma^S{}_{exc}$.

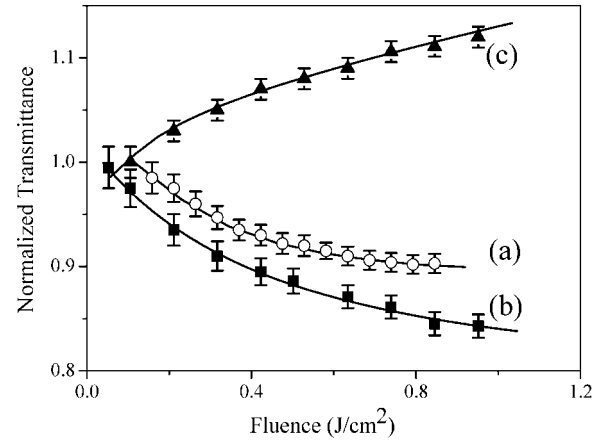

Figure 5. Normalized transmittance as a function of 70 ps pulse fluence for (a) Mn^{3+} $TPPS_4$, (b) Fe^{3+} $TPPS_4$ (pH 9.0), and (c) Fe^{3+} $TPPS_4$ (pH 4.0).

that the S_1 state decays in the picosecond range. In this case, the triplet state is populated during the 70 ps pulse, and the nonlinear absorption can be attributed to simultaneous $S_0 \rightarrow S_1$, $S_1 \rightarrow S_n$, and $T_1 \rightarrow T_n$ transitions. Therefore, we applied the complete five-energy-level diagram to analyze the sample transmittance as a function of pulse fluence. These experiments yielded $\sigma^T{}_{exc}$, τ_{S_1}, and τ_{isc} for Mn^{3+} and Fe^{3+} $TPPS_4$. The values of the cross-sections obtained are presented in Table 1. Zn^{2+} and Mn^{3+} complexes have $\sigma^S{}_{exc}$ and $\sigma^T{}_{exc}$ values 2−4 times higher than that of σ_g. Therefore, Mn^{3+} $TPPS_4$ presents a reverse saturable absorption (RSA) in both femtosecond and picosecond timescales, while Zn^{2+} $TPPS_4$ presents the same behavior for both picosecond and nanosecond ranges. This result is similar to that of free base $TPPS_4$ porphyrin in its nonprotonated form.[15] Fe^{3+} $TPPS_4$ has $\sigma^S{}_{exc}$ 10% higher and $\sigma^T{}_{exc}$ 10% lower than σ_g at pH 4.0. In the femtosecond timescale, it presents a very weak RSA effect, while in the picosecond scale, it demonstrates a very weak saturable absorption (SA) effect. On the other hand, Fe^{3+} $TPPS_4$ presents both $\sigma^S{}_{exc}$ and $\sigma^T{}_{exc}$ higher than σ_g at pH 9.0, producing a RSA behavior in both femtosecond and picosecond timescales. Moreover, since $\sigma^S{}_{exc}$ is 14 times higher than σ_g, the RSA effect is very strong in the femtosecond timescale, making this complex promising for application as an ultrafast optical limiter with femtosecond response time. A similar effect was observed for the free base $TPPS_4$ porphyrin in its protonated form,[15] where both $\sigma^S{}_{exc}$ and $\sigma^T{}_{exc}$ are nearly 9 times higher than σ_g.

TABLE 2: S_1 State Lifetimes (τ_{S_1}), Interconversion (τ_{ic}), and Intersystem Crossing (τ_{isc}) Times and Fluorescence (φ_{fl}), Interconversion (φ_{ic}), and Intersystem Crossing (φ_{isc}) Quantum Yields of Studied Compounds

$TPPS_4$	pH	τ_{S_1} (ps)	τ_{ic} (ps)	τ_{isc} (ps)	φ_{fl}	φ_{ic}	φ_{isc}
free base[17]	4.0	3600 (±100)	13000 (±500)	10000 (±500)	0.37 (±0.06)	0.27 (±0.06)	0.36 (±0.06)
free base[17]	7.0	9700 (±200)	140000 (±1000)	13000 (±500)	0.16 (±0.05)	0.07 (±0.03)	0.77 (±0.09)
Fe^{3+}	4.0	3 (±1)	6 (±1)	6 (±2)	0	0.5 (±0.2)	0.5 (±0.2)
Fe^{3+}	9.0	4 (±1)	12 (±1)	6 (±2)	0	0.3 (±0.2)	0.7 (±0.2)
Mn^{3+}	6.8	4 (±1)	7 (±1)	10 (±2)	0	0.6 (±0.2)	0.4 (±0.2)
Zn^{2+}	6.8	1700 (±100)[17]	7700 (±100)	2300 (±400)	0.04 (±0.01)	0.22 (±0.08)	0.74 (±0.1)

The relaxation times measured and the calculated quantum yields are presented in Table 2. The intersystem crossing quantum yields were calculated from $\varphi_{isc} = \tau_{S_1}/\tau_{isc}$. On the basis of the fact that the fluorescence quantum yields, φ_{fl}, are practically zero in Fe^{3+} $TPPS_4$ and Mn^{3+} $TPPS_4$, we considered that the sum of the interconversion and intersystem crossing quantum yields should be $\varphi_{ic} + \varphi_{isc} = 1$ for the S_1 state deactivation and calculated the interconversion quantum yields and lifetimes, respectively, as $\varphi_{ic} = 1 - \tau_{S_1}/\tau_{isc}$ and $\tau_{ic} = \tau_{S_1}/\varphi_{ic}$.

From quantum yields and lifetimes values obtained, we concluded that the intersystem crossing is the main relaxation path for Zn^{2+} $TPPS_4$ and Fe^{3+} $TPPS_4$ at pH 9.0, while interconversion is the dominant process for Mn^{3+} $TPPS_4$. For Fe^{3+} $TPPS_4$ at pH 4.0, both paths are equivalent. τ_{S_1}, τ_{isc}, and τ_{ic} for Zn^{2+} $TPPS_4$ are in the nanosecond timescale, similar to those found for free-base porphyrin, while for Fe^{3+} and Mn^{3+} $TPPS_4$, these values are ~3 orders of magnitude lower than that of free-base porphyrin.[17] Thus, as opposed to Zn^{2+}, the $TPPS_4$ interaction with Mn^{3+} and Fe^{3+} increases dramatically the probability of both $S_1 \rightarrow S_0$ interconversion and $S_1 \rightarrow T_1$ intersystem crossing.

In porphyrins, $S_0 \rightarrow S_1$ transitions correspond to $\pi \rightarrow \pi^*$ transitions of π electrons in the porphyrin ring. Metalloporphyrins, which contain central ions with a completely filled external shell, such as Zn^{2+}, have a d^{10} electronic configuration. In this case, the role of metal ion electrons in the porphyrin π conjugated system is negligible, and only ring electrons take part in $\pi-\pi^*$ transitions.[21] Similar to free base porphyrins, these porphyrin complexes are named regular.

In contrast to Zn^{2+}, Mn^{3+} and Fe^{3+} have unfilled d and f external shells and possess d^4 and d^5 electronic configurations, respectively. Porphyrin complexes with such ions are known as irregular. In Mn^{3+} porphyrins, four half-filled metal orbitals d_{xy}, d_π(d_{xz} and d_{yz}), and d_{z^2} are localized between two highest filled ring orbitals $a_{1u}(\pi)$ and $a_{2u}(\pi)$ and two lowest empty ring orbitals $e_g(\pi^*)$. The empty metal d_{z2-y2} orbital lies higher than the $e_g(\pi^*)$ orbitals.[21–26] In Fe^{3+} porphyrins, the half-filled d_π and d_{z^2} orbitals also are positioned between porphyrin ring filled π and empty π^* orbitals.[26–29] These metal orbitals are considered as electron acceptors.[26,27] As a result, irregular porphyrins usually present the charge transfer (CT)[21,23] of unpaired metal electron to the ring π conjugated system. This produces a strong reduction of the time of porphyrin π^* state deactivation due to π^* state energy transfer to the CT state.

On the other hand, the presence of paramagnetic metal ions, such as Mn^{3+} and Fe^{3+}, increases the spin-orbit coupling in porphyrin electronic systems, and the electronic states cannot be considered as pure singlet or pure triplet. This weakens the transition prohibition between the electronic states with different spin multiplicities and reduces the excited state lifetimes. The lowest excited singlet state of paramagnetic metalloporphyrins is of singmultiplet character, and this state couples efficiently to tripmultiplet states, resulting in rapid intersystem crossing to the triplet manifold. For Mn^{3+} porphyrins, the existence of two tripmultiplet levels was suggested: a short-lived tripquintet, relaxing to a long-lived tripseptet $^5T_1(\pi-\pi^*) \rightarrow {}^7T_1(\pi-\pi^*)$.[22] For iron porphyrins, the fast deactivation of π^* states occurs via a tripsextet to a tripoctet transition $^6T_1(\pi-\pi^*) \rightarrow {}^8T_1(\pi-\pi^*)$.[23] The π^* state intermolecular quenching due to energy transition to tripmultiplets is supposedly more probable than that via the CT state.[22]

Conclusion

We determined the $S_1 \rightarrow S_n$ and $T_1 \rightarrow T_n$ transition cross-sections of $TPPS_4$ complexes with Zn^{2+}, Fe^{3+}, and Mn^{3+} as well as the characteristic interconversion and intersystem crossing times and quantum yields of their S_1 state. The five-energy-level diagram was employed to describe the excited state dynamics. We observed that Fe^{3+} and Mn^{3+} reduce deactivation times by 3 orders of magnitude, while the effect of Zn^{2+} was much smaller. This difference was attributed to Fe^{3+} and Mn^{3+} open-shell electronic configurations and to the closed-shell Zn^{2+} structure. Zn^{2+} $TPPS_4$ presents a RSA effect in picosecond and nanosecond regimes, with accumulative contribution in the latter case. Fe^{3+} and Mn^{3+} $TPPS_4$ complexes do not present accumulative effects, which means that the excited state deactivation is ultrafast in these complexes due to metal−porphyrin CT and the increase of spin-electron coupling in the porphyrin π conjugated electronic system. The femtosecond excitation yields RSA effects for Mn^{3+} $TPPS_4$ and Fe^{3+} $TPPS_4$ at pH 9.0 and a SA effect for Fe^{3+} $TPPS_4$ at pH 4.0. We found that σ^S_{exc} is 14 times higher than σ_g for Fe^{3+} $TPPS_4$ at pH 9.0, which is important for optical limiting in the picosecond regime. We also observed that intersystem crossing is the main relaxation mechanism for Fe^{3+} and Zn^{2+} $TPPS_4$, while interconversion is the dominant process for Mn^{3+} $TPPS_4$.

Acknowledgment. The Fundação de Amparo à Pesquisa do Estado de São Paulo is thanked for financial support.

References and Notes

(1) Bonnett, R. *Chem. Soc. Rev.* **1995**, *24*, 19.
(2) Ochsner, M. *J. Photochem. Photobiol.* **1997**, *39*, 1.
(3) Klein, A. T. J.; Rosh, F.; Coenen, H. H.; Qaim, S. M. *Appl. Radiat. Isotopes* **2005**, *62*, 711.
(4) Yushmanov, V. E.; Tominaga, T. T.; Borissevitch, I. E.; Imasato, H.; Tabak, M. *Magn. Reson. Imaging* **1996**, *14*, 255.
(5) Calvete, M.; Yang, C. Y.; Hanack, M. *Synth. Met.* **2004**, *141*, 231.
(6) Singh, C. P.; Bindra, K. S.; Jain, B.; Oak, S.M. *Opt. Commun.* **2005**, *245*, 407.
(7) Liu, M. O.; Tai, C.-H.; Hu, A. T.; Wei, T.-H. *J. Organomet. Chem.* **2004**, *689*, 2138.
(8) Liu, Y. L.; Liu, Z. B.; Tian, J. G.; Zhu, Y.; Zheng, J. Y. *Opt. Commun.* **2008**, *281*, 776.
(9) Senge, M. O.; Fazekas, M.; Notaras, E. G. A.; Blau, W. J.; Zawadzka, M.; Locos, O. B.; Mhuircheartaigh, E. M. N. *Adv. Mater.* **2007**, *19*, 2737.
(10) Jiang, L.; Jiu, T.; Li, Y.; Li, Y.; Yang, J.; Li, J.; Li, C.; Liu, H.; Song, Y. *J. Phys. Chem. B* **2008**, *112*, 756.

(11) McEwan, K.; Lewis, K.; Yang, G. Y.; Chng, L. L.; Lee, Y. W.; Lau, W. P.; Lai, K. S. *Adv. Funct. Mater.* **2003**, *13*, 863.

(12) Gandini, S. C. M.; Yushmanov, V. E.; Perussi, J. R.; Tabak, M.; Borissevitch, I. E. *J. Inorg. Biochem.* **1999**, *73*, 35.

(13) Borissevitch, I. E.; Bezerra, A. G., Jr.; Gomes, A. S. L.; de Araujo, R. E.; de Araújo Cid, B.; Oliveira, K. M. T.; Trsic, M. *J. Porphyrins Phthalocyanines* **2001**, *5*, 51.

(14) Sheik-Bahae, M.; Said, A. A.; van Stryland, E. W. *Opt. Lett.* **1989**, *14*, 955.

(15) Gonçalves, P. J.; De Boni, L.; Barbosa Neto, N. M.; Rodrigues, J. J., Jr.; Zílio, S. C.; Borissevitch, I. E. *Chem. Phys. Lett.* **2005**, *407*, 236.

(16) Wei, T.-H.; Huang, T.-H.; Wen, T.-C. *Chem. Phys. Lett.* **1999**, *314*, 403.

(17) Gonçalves, P. J.; Aggarwal, L. P. F.; Marquezin, C. A.; Ito, A. S.; De Boni, L.; Barbosa Neto, N. M.; Rodrigues, J. J., Jr.; Zílio, S. C.; Borissevitch, I. E. *J. Photochem. Photobiol., A* **2006**, *181*, 378.

(18) Barbosa Neto, N. M.; De Boni, L.; Mendonca, C. R.; Misoguti, L.; Queiroz, S. L.; Dinelli, L. R.; Batista, A. A.; Zílio, S. C. *J. Phys. Chem. B* **2005**, *109*, 17340.

(19) Barbosa Neto, N. M.; Oliveira, S. L.; Misoguti, L.; Mendonca, C. R.; Gonçalves, P. J.; Borissevitch, I. E.; Dinelli, L. R.; Romualdo, L. L.; Batista, A. A.; Zílio, S. C. *J. Appl. Phys.* **2006**, *99*, 123103.

(20) Misoguti, L.; Mendonça, C. R.; Zílio, S. C. *Appl. Phys. Lett.* **1999**, *74*, 1531.

(21) Kalyanasundatam, K. *Photochemistry of Polypyridine and Porphyrin Complexes*; Academic Press: San Diego, 1992.

(22) Yan, X.; Kirmaier, C.; Holten, D. *Inorg. Chem.* **1986**, *25*, 4774.

(23) Harriman, A. *J. Cem. Soc., Faraday Trans. 1* **1981**, *77*, 369.

(24) Humphrey, J. L.; Kuciauskas, D. *J. Am. Chem. Soc.* **2006**, *128*, 3902.

(25) Kim, Y.; Choi, J. R.; Yoon, M; Furube, A.; Asahi, T.; Masuhara, H. *J. Phys. Chem. B* **2001**, *105*, 8513.

(26) Rodriguez, J.; Holten, D. *J. Chem. Phys.* **1989**, *91*, 3525.

(27) Sorgues, S.; Poisson, L.; Raffael, K.; Krim, L.; Soep, B.; Shafizadeh, N. *J. Chem. Phys.* **2006**, *124*, 114302.

(28) Humphrey, J. L.; Kuciauskas, D. *J. Phys. Chem. C* **2008**, *112*, 1700.

(29) Liao, M.-S.; Scheiner, S. *J. Chem. Phys.* **2002**, *117*, 205.

JP800589J